



## The role and position of iron in $0.8\text{CaZrO}_3\text{-}0.2\text{CaFe}_2\text{O}_4$

Jacek Szczerba,  
Edyta Śnieżek,  
Paweł Stoch,  
Ryszard Prorok,  
Ilona Jastrzębska

**Abstract.** The aim of the study was to characterize the  $0.8\text{CaZrO}_3\text{-}0.2\text{CaFe}_2\text{O}_4$  composite structure with particular emphasis on the role and position of iron in the function of sintering temperature. The paper presents the results of  $^{57}\text{Fe}$  Mössbauer effect at room temperature. It was found that the increase of sintering temperature causes an increase in the amount of incorporated iron ions in the  $\text{CaZrO}_3$ -crystal structure. Based on Mössbauer spectroscopy analysis, it was found that three different environments of  $\text{Fe}^{3+}$  ions were observed in the obtained materials. Two of them corresponded to  $\text{CaFe}_2\text{O}_4$  phase and one was associated with the substitution of  $\text{Zr}^{4+}$  by  $\text{Fe}^{3+}$  in the  $\text{CaZrO}_3$  structure.

**Key words:** calcium ferrite • calcium zirconate • Mössbauer spectroscopy • perovskite • spinel

### Introduction

$\text{CaZrO}_3$  is a member of perovskite, which has two polymorphs. At temperatures lower than  $1750^\circ\text{C}$ , an orthorhombic phase is stable, where  $\text{Ca}^{2+}$  ions are situated between slightly deformed  $\text{ZrO}_6$  octahedrals. At temperatures higher than  $1750^\circ\text{C}$ , cubic phase is stable [1, 2]. High purity  $\text{CaZrO}_3$  can be obtained by the arc melting technique. The fused  $\text{CaZrO}_3$ , with strong Zr-O covalent bonding and almost pure Ca-O ionic bonding, is poreless and has the density close to the theoretical one [3].

$\text{CaZrO}_3$ , which is the only chemical compound in the CaO-ZrO<sub>2</sub> binary system, is characterized by high melting point ( $2345^\circ\text{C}$ ), thermal shock resistance, high strength and corrosion resistance against alkali oxides and cement clinker. Furthermore,  $\text{CaZrO}_3$  has been widely investigated because of its electrical properties.  $\text{CaZrO}_3$  is a p-type semiconductor. Modified by some trivalent cations (e.g.  $\text{In}^{3+}$ ,  $\text{Ga}^{3+}$  and  $\text{Sc}^{3+}$ ) is a protonic conductor in hydrogen atmosphere. Small excess of zircona or calcia in  $\text{CaZrO}_3$  structure cause oxygen ion conductivity. The analogous situation occurs in the case of  $\text{Al}_2\text{O}_3$ ,  $\text{MgO}$ ,  $\text{Y}_2\text{O}_3$  substitution. Therefore,  $\text{CaZrO}_3$  is a material being used as, for example, mechanical filters, resonators, capacitors, and refractory materials [4–10].  $\text{CaZrO}_3$  relatively easily incorporates actinides into its crystal structure.  $\text{CaZrO}_3$  is considered as a host material for spent nuclear fuel immobilization [11].

J. Szczerba, E. Śnieżek✉, P. Stoch, R. Prorok,  
I. Jastrzębska  
Department of Ceramics and Refractories,  
Faculty of Materials Science and Ceramics,  
AGH – University of Science and Technology,  
30 A. Mickiewicza Ave., 30-059 Kraków, Poland,  
Tel.: +48 12 617 5139, Fax: +48 12 633 4630,  
E-mail: esniezek@agh.edu.pl

Received: 18 June 2014  
Accepted: 2 November 2014

$\text{CaFe}_2\text{O}_4$  with spinel structure is stable up to  $1228^\circ\text{C}$  [12]. Crystal structure of  $\text{CaFe}_2\text{O}_4$  is similar to the one formed in perovskite compounds as in  $\text{CaZrO}_3$  [13]. Therefore, it is interesting to study the  $0.8\text{CaZrO}_3\text{-}0.2\text{CaFe}_2\text{O}_4$  composite, which is the combination of perovskite and spinel structure compounds. This work is focused on determining the position of the iron in the studied composite depending on the synthesis temperature.

## Experiment

The  $0.8\text{CaZrO}_3\text{-}0.2\text{CaFe}_2\text{O}_4$  composite was synthesized by solid-state reaction, starting from pure  $\text{CaCO}_3$ ,  $\text{ZrO}_2$ , and  $\text{Fe}_2\text{O}_3$  commercial powders. Synthesis of the material was achieved by a two-step heating process. The first step at  $1200^\circ\text{C}$  was calcination. The recovered material was grounded and pressed under 30 MPa before the second step heat treatment at  $1400^\circ\text{C}$  and  $1700^\circ\text{C}$  with the 10 h soaking time at each temperature.

The X-ray diffraction analysis was performed at a room temperature, using monochromatic  $\text{Cu-K}\alpha$  radiation (Philips Panalytical X'Pert-Pro MPD diffractometer) in order to determine the phase composition of the fired materials. The crystal structure parameters were obtained using the full-profile Rietveld method [14] implemented in the FullProf software package [15].

The  $^{57}\text{Fe}$  Mössbauer effect measurements were performed using the standard technique at room temperature in transmission mode, using a conventional constant-acceleration spectrometer and a 25 mCi  $^{57}\text{Co}$  source in Rh matrix. The velocity scale was calibrated using  $\alpha\text{-Fe}$  foil. Spectra were fitted to Lorentzian lines using the non-linear least square method.

## Results and discussion

Figure 1 shows X-ray diffraction (XRD) patterns and theoretical fits of the samples sintered at  $1400^\circ\text{C}$  and  $1700^\circ\text{C}$ . It was found that the main crystalline phases were  $\text{CaZrO}_3$  ( $Pcmm$ ) and  $\text{CaFe}_2\text{O}_4$  ( $Pnam$ ).

**Table 1.** Crystal structure parameters of  $\text{CaZrO}_3$  and  $\text{CaFe}_2\text{O}_4$  phases (a, b, c – unit cells parameters, V – unit cell volume, A – phase share percentage)

Parameters	Sintering temperature		JCPDS
	$1400^\circ\text{C}$	$1700^\circ\text{C}$	
$\text{CaZrO}_3$ ( $Pcmm$ )			
a [Å]	5.586(1)	5.582(1)	5.5912
b [Å]	8.011(1)	8.007(1)	8.0171
c [Å]	5.754(1)	5.754(1)	5.7616
V [Å <sup>3</sup> ]	257.54(1)	257.22(1)	258.26
A [%]	92.6(9)	88.0(9)	
$\text{CaFe}_2\text{O}_4$ ( $Pnam$ )			
a [Å]	10.756(9)	10.732(9)	10.705
b [Å]	9.262(4)	9.261(4)	9.23
c [Å]	3.027(4)	3.026(4)	3.024
V [Å <sup>3</sup> ]	301.56(7)	300.86(7)	298.79
A [%]	7.4(6)	12.0(6)	

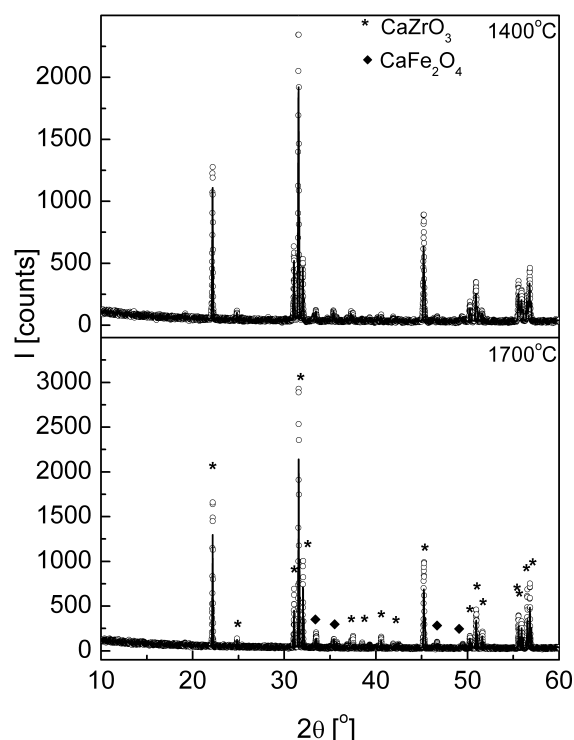


**Fig. 1.** X-ray diffraction patterns and the Rietveld analysis of the samples sintered at  $1400^\circ\text{C}$  and  $1700^\circ\text{C}$ .

Parameters of both the crystalline phases are summarized in Table 1. With the sintering temperature increases the amount of the  $\text{CaFe}_2\text{O}_4$  phase at the cost of  $\text{CaZrO}_3$ , which could indicate the dissolution of  $\text{CaZrO}_3$  by  $\text{CaFe}_2\text{O}_4$  liquid phase. At both temperatures, a reduction of unit cell volume of  $\text{CaZrO}_3$  is observed. It may be caused by diffusion and incorporation of  $\text{Fe}^{3+}$  cations, which replaced bigger  $\text{Zr}^{4+}$  cations in the perovskite structure. An effective ionic radius of  $\text{Zr}^{4+}$  (0.72 Å) is considerably bigger than  $\text{Fe}^{3+}$  (0.55 Å) [16]. Thus if part of Zr is substituted by Fe, it should decrease the crystal structure parameters. The opposite effect is observed in the case of  $\text{CaFe}_2\text{O}_4$ . The diffusion and incorporation process are thermally activated. Therefore, at  $1700^\circ\text{C}$  in comparison to  $1400^\circ\text{C}$ , the lowest parameters of unit cell were obtained.

**Table 2.** The hyperfine interaction parameters (A – area of the subspectra, IS – isomer shift, QS – quadrupole split) of the sample prepared at 1400°C and 1700°C

Component	A [%]	IS [mm/s]	QS [mm/s]
1400°C			
1	63.7	0.338(4)	0.647(7)
2	28.5	0.364(1)	0.322(5)
3	7.8	0.437(5)	0.643(8)
1700°C			
1	54.4	0.313(16)	0.627(10)
2	26.1	0.353(1)	0.305(13)
3	19.5	0.429(9)	0.633(10)

The results of the Mössbauer spectroscopy measurements are shown in Fig. 2 and are summarized in Table 2. It was found that the obtained spectra are the result of three components, which correspond to the three different neighborhoods of Fe<sup>3+</sup> ions. In the case of components 1 and 2, the hyperfine interaction parameters correspond to pure CaFe<sub>2</sub>O<sub>4</sub> [17], where iron occurs in the octahedral and tetrahedral sites (approximately 2:1 contribution). In contrast, component 3 is derived from iron, which was incorporated into the CaZrO<sub>3</sub> structure and replaces zircon in octahedral sites. The substitution of Zr<sup>4+</sup>/Fe<sup>3+</sup> causes an imbalance of a cell charge. This is compensated by the presence of an oxygen octahedron distortion in the middle of which Fe<sup>3+</sup> cations are situated, or by the removal of one oxygen unit from an octahedron corner. Its coordination number declines from 6 to 5. This effect causes the appearance of the larger electric field gradient acting on the Fe<sup>3+</sup> ions, which leads to an increase of quadrupole splitting (QS) parameter. The increase of the sintering temperature causes the increase in

incorporation of Fe<sup>3+</sup> ions into the CaZrO<sub>3</sub> structure from approximately 8% to 20%.

### Conclusions

The aim of the study is to characterize the 0.8CaZrO<sub>3</sub>-0.2CaFe<sub>2</sub>O<sub>4</sub> composite structure based on calcium zirconate with calcium ferrite in the matrix, with particular emphasis on the role and position of iron, as a function of temperature synthesis. Parameters of both the obtained crystalline phases: CaZrO<sub>3</sub> and CaFe<sub>2</sub>O<sub>4</sub> are slightly different, compared to the reference data, which may indicate the incorporation of iron in the CaZrO<sub>3</sub> crystal structure and zirconium in CaFe<sub>2</sub>O<sub>4</sub>. With the increase of the sintering temperature, a gradual dissolution of CaZrO<sub>3</sub> in the CaFe<sub>2</sub>O<sub>4</sub> liquid phase is observed. It was found that the sintering temperature increase causes an increase in the incorporation of iron ions into the crystal structure of calcium zirconate from approximately 8% to 20%. The study revealed that the CaZrO<sub>3</sub> structure is able to embody up to about 2 mol% of Fe<sup>3+</sup>.

**Acknowledgment.** The work was supported by the grant no. INNOTECH-K2/IN2/16/181920/NCBR/13.

### References

1. Dravid, V. P., Sung, C. M., Notis, M. R., & Lyman, C. E. (1989). Crystal symmetry and coherent twin structure of calcium zirconate. *Acta Crystallogr. Sect. B-Struct. Sci.*, 45(3), 218–227. DOI: 10.1107/S0108768189000856.
2. Rossa, N. L., & Chaplin, T. D. (2003). Compressibility of CaZrO<sub>3</sub> perovskite: Comparison with Ca-oxide perovskites. *J. Solid State Chem.*, 172(1), 123–126. DOI: 10.1016/S0022-4596(02)00166-4.
3. Stoch, P., Szczerba, J., Lis, J., Madej, D., & Pędzich, Z. (2012). Crystal structure and *ab initio* calculations of CaZrO<sub>3</sub>. *J. Eur. Ceram. Soc.*, 32(3), 665–670. DOI: 10.1016/j.jeurceramsoc.2011.10.011.
4. Prasanth, C. S., Padma Kumar, H., Pazhani, R., Solomon, S., & Thomas, J. K. (2008). Synthesis, characterization and microwave dielectric properties of nanocrystalline CaZrO<sub>3</sub> ceramics. *J. Alloy. Compd.*, 464(1/2), 306–309. DOI: 10.1016/j.jallcom.2007.09.098.

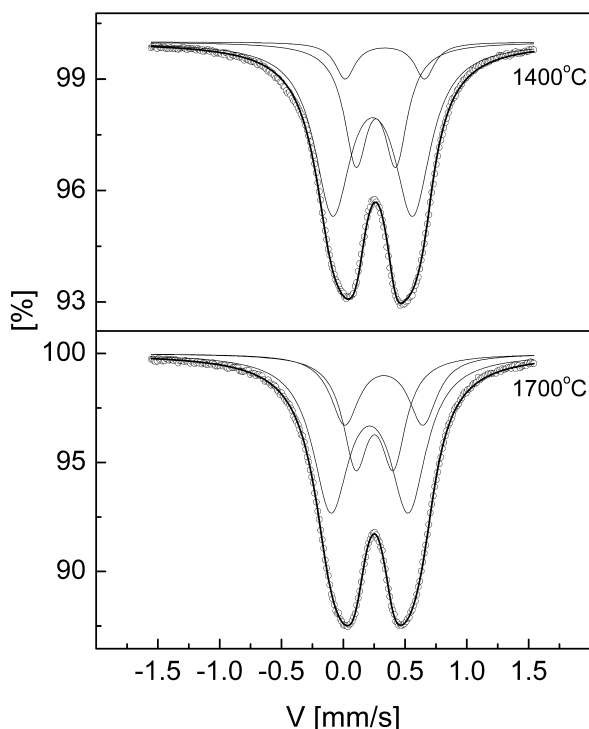


**Fig. 2.** <sup>57</sup>Fe Mössbauer effect measurements at room temperature of the sample sintered at 1400°C and 1700°C.

5. Pollet, M., Marinel, S., & Desgardin, G. (2004). CaZrO<sub>3</sub>, a Ni-co-sinterable dielectric material for base metal-multilayer ceramic capacitor applications. *J. Eur. Ceram. Soc.*, 24(1), 119–127. DOI: 10.1016/S0955-2219(03)00122-5.
6. Levin, I., Amos, T. B., Bell, S. M., Farber, L., Vanderah, T. A., Roth, R. S., & Toby, B. H. (2003). Phase equilibria, crystal structures, and dielectric anomaly in the BaZrO<sub>3</sub>-CaZrO<sub>3</sub> system. *J. Solid State Chem.*, 175, 170–181. DOI: 10.1016/S0022-4596(03)00220-2.
7. Serena, S., Sainz, M. A., & Caballero, A. (2009). The system Clinker-MgO-CaZrO<sub>3</sub> and its application to the corrosion behavior of CaZrO<sub>3</sub>/MgO refractory matrix by clinker. *J. Eur. Ceram. Soc.*, 29(11), 2199–2209. DOI: 10.1016/j.jeurceramsoc.2009.01.015.
8. Dudek, M., & Bućko, M. M. (2003). Electrical properties of stoichiometric and non-stoichiometric calcium zirconate. *Solid State Ion.*, 157, 183–187.
9. Dudek, M., & Drożdż-Cieśla, E. (2009). Some observations on synthesis and electrolytic properties of nonstoichiometric calcium zirconate. *J. Alloy. Compd.*, 457, 846–854. DOI: 10.1016/j.jallcom.2008.08.020.
10. Hwang, S. C., & Choi, G. M. (2006). The effect of cation nonstoichiometry on the electrical conductivity of acceptor-doped CaZrO<sub>3</sub>. *Solid State Ion.*, 177, 3099–3103. DOI: 10.1016/j.ssi.2006.08.002.
11. Smith, K. L., Colella, M., Cooper, R., & Vance, E. R. (2003). Measured displacement energies of oxygen ions in titanates and zirconates. *J. Nucl. Mater.*, 321(1), 19–28. DOI: 10.1016/S0022-3115(03)00197-1.
12. Muller-Buschbaum, H. K. (2003). The crystal chemistry of AM<sub>2</sub>O<sub>4</sub> oxometallates. *J. Alloy. Compd.*, 349(1/2), 49–104.
13. Muller, O., & Roy, R. (1974). *The major ternary structural families*. New York: Springer.
14. Rietveld, H. M. (1969). A profile refinement method for nuclear and magnetic structures. *J. Appl. Cryst.*, 2, 65–71. DOI: 10.1107/S0021889869006558.
15. Rodriguez-Carvajal, J. (1993). Recent advances in magnetic structure determination by neutron powder. *Diffr. Phys. B*, 192(1/2), 55–69. DOI: 10.1016/0921-4526(93)90108-I.
16. Shannon, R. D. (1976). Revised effective ionic radii and systematic studies of interatomic distances in halides and chalcogenides. *Acta Crystallogr. Sect. A*, 32, 751–767. DOI: 10.1107/S0567739476001551.
17. Tsipis, E. V., Pivak, Y. V., Waerenborgh, J. C., Kolotygin, V. A., Viskup, A. P., & Khortan, V. V. (2007). Oxygen ionic conductivity, Mössbauer spectra and thermal expansion of CaFe<sub>2</sub>O<sub>4-δ</sub>. *Solid State Ion.*, 178(25/26), 1428–1436. DOI: 10.1016/j.ssi.2007.09.003.